Jpn. J. Appl. Phys. Vol. 39 (2000) pp. 4438–4442
Part 1, No. 7B, July 2000

Substrate-Structure Dependence of Ag Electromigration on Au-Precovered Si(111) Surfaces

Fangxiao SHI[1,2], Ichiro SHIRAKI[1], Tadaaki NAGAO[1,2] and Shuji HASEGAWA[1,2,*]

[1]*Department of Physics, University of Tokyo, Hongo 7-3-1, Bunkyo-ku, Tokyo 113-0033, Japan*
[2]*Core Research for Evolutional Science and Technology, Japan Science and Technology Corporation, 4-1-8 Honcho, Kawaguchi, Saitama 332-0012, Japan*

(Received December 29, 1999; accepted for publication January 27, 2000)

Electromigration of Ag on Au-precovered Si(111) surfaces was investigated by *in-situ* ultrahigh vacuum scanning electron microscopy and μ-probe reflection-high-energy electron diffraction (RHEED). Migration behaviors of a Ag-film patch strongly depended on Au coverage θ_{Au} and corresponding surface structures. When $\theta_{\mathrm{Au}} < 0.7$ monolayer (ML), the patch expanded preferentially towards the cathode to attain a maximum area in which the sum of Ag and Au coverages were always about 1 ML irrespective of θ_{Au}, resulting in two-dimensional (2D) alloy phases (showing $\sqrt{3} \times \sqrt{3}$ RHEED patterns) with different Au/Ag concentration ratios. The largest expansion of the patch area was achieved on a $(5 \times 2 + \alpha\text{-}\sqrt{3} \times \sqrt{3})$-Au mixed phase structure ($\theta_{\mathrm{Au}} \sim 0.7$ ML). However, when $\theta_{\mathrm{Au}} > 0.7$ ML, the patch expansion was greatly reduced. Especially on the β-$\sqrt{3} \times \sqrt{3}$-Au surface ($\theta_{\mathrm{Au}} \sim 1.0$ ML), the patch showed no directional expansion towards the cathode. But Ag atoms were observed to migrate inside the patches on all substrates (including the β-$\sqrt{3} \times \sqrt{3}$-Au surface) to form 3D islands near terrace edges.

KEYWORDS: silicon surface, electromigration, surface superstructure, scanning electron microscopy, surface migration, alloy

The electromigration on semiconductor surfaces has attracted considerable interest over the past decade. It has been widely observed in thin metal films,[1–6] metal islands,[7] Si adatoms[8–12] and Si microclusters[13] on Si(111) or Si(001) substrates, and proved to be an important surface mass transport phenomenon, which is both physically interesting and technologically important. However, so far, few results have been reported on the migration of metals on differently modified surfaces or the migration of alloy adsorbates. Since Au can cause a variety of superstructures on Si(111) surfaces upon submonolayer deposition,[14,15] and since Au and Ag move in opposite directions due to electromigration on a clean Si(111) surface,[1] it will be instructive to observe the Ag migration on Au-precovered Si surfaces with various Au coverages for the purpose of understanding the mechanism of electromigration. In this paper, we investigate the migration by means of *in-situ* scanning electron microscopy (SEM) and μ-probe reflection-high-energy electron diffraction (RHEED).

The experiments were carried out in an ultrahigh vacuum chamber equipped with a Hitachi S-4200 field emission SEM column and μ-probe RHEED. The base pressure in the chamber was 2×10^{-8} Pa, and during deposition it was maintained below 1×10^{-7} Pa. The substrate ($15 \times 4 \times 0.4\,\mathrm{mm}^3$ in size) was cut from an *n*-type Si(111) wafer (50–100 Ω·cm), with its longer side parallel to the $\langle 1\bar{1}0 \rangle$ direction. After flash cleaning at 1473 K for 1 min and annealing around 1073 K for 3 min by passing direct current through the substrate, a clean 7×7 surface was obtained. Current direction was always selected to obtain a step-bunched surface. First, a controlled amount of Au was deposited from an alumina-coated tungsten basket onto the entire Si surface at a substrate temperature of 873 K to prepare the Au-induced surface superstructures. Then Ag of 5.3 ± 0.5 monolayer (ML) thickness was deposited through a Mo mask (with a rectangular window whose width was 150 μm) onto a central part of the Si surface at room temperature (RT) to fabricate a Ag-film patch. One ML corresponds to 7.8×10^{14} atoms/cm^2. Electromigration measurements were performed by applying direct current to the sample along the $\langle 1\bar{1}0 \rangle$ direction with maintaining the substrate temperature constant between 723 K–813 K, at which very little electromigration of Au was expected. The acceleration voltage of SEM was 30 kV and the electron beam diameter on the sample surface was $\sim$2 nm. The glancing angle of the incident electron beam was about 10° from the surface, so the SEM images shown here suffer from foreshortening in vertical direction.

Figure 1(a) shows a Ag-film patch of about 5.3 ML thickness deposited on the clean 7×7 surface at RT, exhibiting parallel step bunches (where about 40 bilayer steps are accumulated) with about 10 μm spacing. Figure 1(b) was taken after feeding a current of 0.42 A for 10 min at 813 K, showing a preferential spread of the patch towards the cathode. White arrowheads shown in the images can be used as markers for evaluating the migration of the patch. Figures 1(c) and 1(e) depict as-deposited Ag patches on a mixed phase of 5×2-Au and α-$\sqrt{3} \times \sqrt{3}$-Au (Au coverage $\theta_{\mathrm{Au}} \sim 0.71$ ML) (abbreviated to $(5 \times 2 + \alpha\text{-}\sqrt{3})$ hereafter, similarly use for β-$\sqrt{3}$), and on a single phase of β-$\sqrt{3}$ ($\theta_{\mathrm{Au}} \sim 1.0$ ML) at RT, respectively, and 1(d) and 1(f) are the images after current stressing. The patch spreads anisotropically on the $(5 \times 2 + \alpha\text{-}\sqrt{3})$ substrate as on the 7×7 substrate, while the patch on the β-$\sqrt{3}$ substrate shows no spreading even with much longer current-stressing duration.

The electromigration of Au on a clean Si(111) surface has been reported by two groups of researchers.[1,5] Though the general features of the migrations are similar to each other, there is a controversial issue between them. Yasunaga and Natori's study by scanning Auger microscopy[1] shows that directional migration starts at 1.0 ML Au coverage (β-$\sqrt{3}$ structure). However, the result obtained by Yagi *et al*. by reflection electron microscopy observation[5] indicates that the directional movement can take place only after Au coverage is reduced below 0.76 ML (5×2 domains occur), and Au atoms on the $\sqrt{3}$ structure do not show electromigration, which is attributed to the difference in electronic states between the $\sqrt{3}$ and 5×2 structures. Our present result of Ag migration on the Au-precovered Si surface, in some respects, corresponds

*Corresponding author. E-mail address: shuji@surface.phys.s.u-tokyo.ac.jp

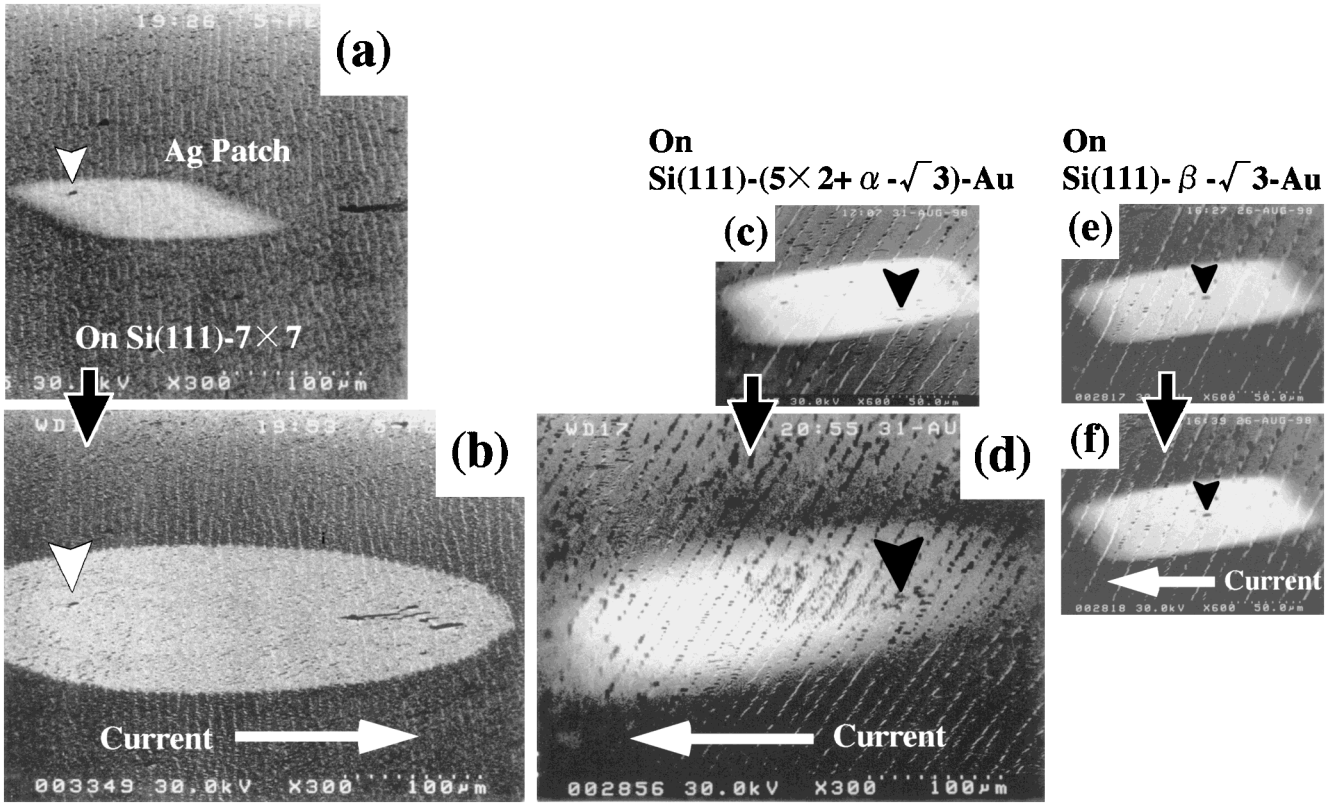

Fig. 1. SEM images showing Ag film patches (a) (c) (e) before and (b) (d) (f) after electromigration (a) (b) on the clean 7×7 surface ($\theta_{Au} = 0$ ML) with 0.42 A for 10 min, (c) (d) on the $(5 \times 2 + \alpha\text{-}\sqrt{3})$ surface ($\theta_{Au} = 0.71$ ML) with 0.35 A for 5 min, and (e) (f) on the $\beta\text{-}\sqrt{3}$ surface ($\theta_{Au} = 1.0$ ML) with 0.35 A for 15.5 min, at 813 K. Arrowheads in the respective images are characteristic defects used for markers.

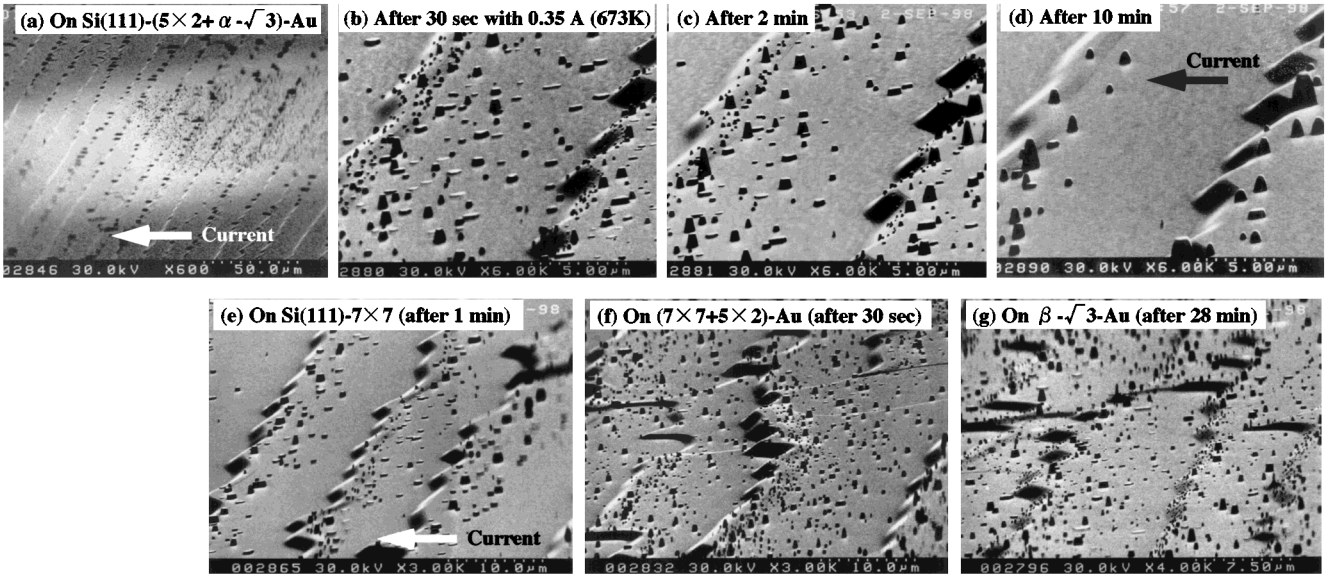

Fig. 2. (a) SEM images showing 3D islands formed inside the patches during current stressing on the $(5 \times 2 + \alpha\text{-}\sqrt{3})$ substrate for 0.5 min at 673 K, (b) its magnified image, (c) and (d) after current stressing for 2 and 10 min, respectively. Similar observations on the (e) 7×7 (for 1 min), (f) $7 \times 7 + 5 \times 2$ (for 0.5 min), and (g) $\beta\text{-}\sqrt{3}$ surfaces (for 28 min). The current is fed from the right to left in the images.

to that of Yagi *et al.*

Figure 2(a) is an SEM image of the Ag patch during current stressing on the $(5 \times 2 + \alpha\text{-}\sqrt{3})$ substrate, and Fig. 2(b) is its magnified image showing three-dimensional (3D) islands inside the patch area appearing by current stressing (and resultant heating). These 3D islands appeared only in the area of the original Ag patch, and not in the extended area of the patch as seen in Fig. 2(a). Flat and tall islands are observed to coexist. Figures 2(c) and 2(d) show images taken after longer duration of current stressing than in Fig. 2(b). It is noted that with extension of current-stressing time, the islands grow larger and accumulate only near the upper sides of bunched

steps. Flat islands tend to disappear and tall islands remain in the later stages. These tall islands also disappeared completely by further current stressing.

Figure 2(e)–2(g) show 3D islands on the other substrates. Their shapes and distributions seem similar to each other. Therefore, it is suggested that, by considering that the 3D islands formed on the 7×7 substrate without Au in Fig. 2(e) are composed of Ag only, the islands on the other substrates are also Ag islands, not Ag–Au alloy ones. On the other hand, round-shaped islands without flat tops appeared when Au of monolayer regimes was deposited on top of the $\sqrt{3} \times \sqrt{3}$-Ag surface following annealing (not shown here), indicating that these islands were presumably of Au–Ag alloy, which could be distinguished from the islands observed in Fig. 2. Behavior of the islands shown in Figs. 2(e)–2(g) with current stressing was also observed to be similar to the case of Figs. 2(c) and 2(d). When the current was applied in a step-up (step-down) direction, the islands were accumulated at the lower side (upper side) of the bunched steps on every substrate. Since the bunched steps are not only barriers against migration but also favorable desorption sites for Ag atoms, it is reasonable to assume that Ag atoms migrate on terraces to be accumulated near step bunches, resulting in an increase in density of the Ag atoms beyond the supersaturation density to form the 3D islands. It should be noted here that although no directional spread of the patch was observed on the β-$\sqrt{3}$ substrate (Fig. 1(f)), Ag atoms migrate towards the cathode within the patch to be accumulated into the 3D islands on the substrate (Fig. 2(g)). However, these Ag atoms do not contribute to the patch expansion, rather desorb from (or diffuse into) the substrate.

Figure 3 shows the migration distance of the front edge of the patch towards the cathode as a function of current-stressing duration at different temperatures, measured from the SEM images like those of Fig. 1 on different substrates. Figure 3(a) clearly indicates that the migration markedly depends on the substrate surface structure. Compared with that on the 7×7 clean substrate, the Ag migration is enhanced on the 5×2 and $(5 \times 2 + \alpha\text{-}\sqrt{3})$ substrates (θ_{Au} is less than $\sim$0.71 ML), but suppressed on the α- and β-$\sqrt{3}$ substrates (θ_{Au} is above $\sim$0.8 ML). The patch exhibits the largest migration on the $(5 \times 2 + \alpha\text{-}\sqrt{3})$ substrate ($\theta_{\mathrm{Au}} \sim 0.71$ ML), while the migration distance is the smallest on the β-$\sqrt{3}$ surface. By comparing the migration distance of the patch at both the anode and cathode sides on the β-$\sqrt{3}$ substrate, we confirmed that the patch extended equally to both sides during current application, indicating only isotropic thermal diffusion. It should be noted that although the maximum migration distances are enhanced on the substrates of $\theta_{\mathrm{Au}} < 0.71$ ML, their initial speed of migration is suppressed compared with that on the 7×7 substrate. Figures 3(b) and 3(c) show the results of similar observations at 763 K and 723 K which only involve three kinds of substrate structures.

Expansion of the patch area by current stressing was measured from SEM images on the different substrates at 813 K. The results are summarized in Fig. 4(a) as a function of the precovered Au coverage, in which the ratios between the patch area after 3D islands apparently disappear and that of the original Ag patch are presented on a solid line with solid squares. On some surfaces, the patch still continued to expand even after the 3D islands apparently disappeared. In such cases, the area ratios when the patch reached its maximum were also measured, and are presented with solid circles on a dashed line in Fig. 4(a). An obvious trend is that the patch expands to the maximum at $\theta_{\mathrm{Au}} \sim 0.7$ ML (on the $(5 \times 2 + \alpha\text{-}\sqrt{3})$ substrate). On the other hand, Ag cannot effectively spread with higher Au coverage.

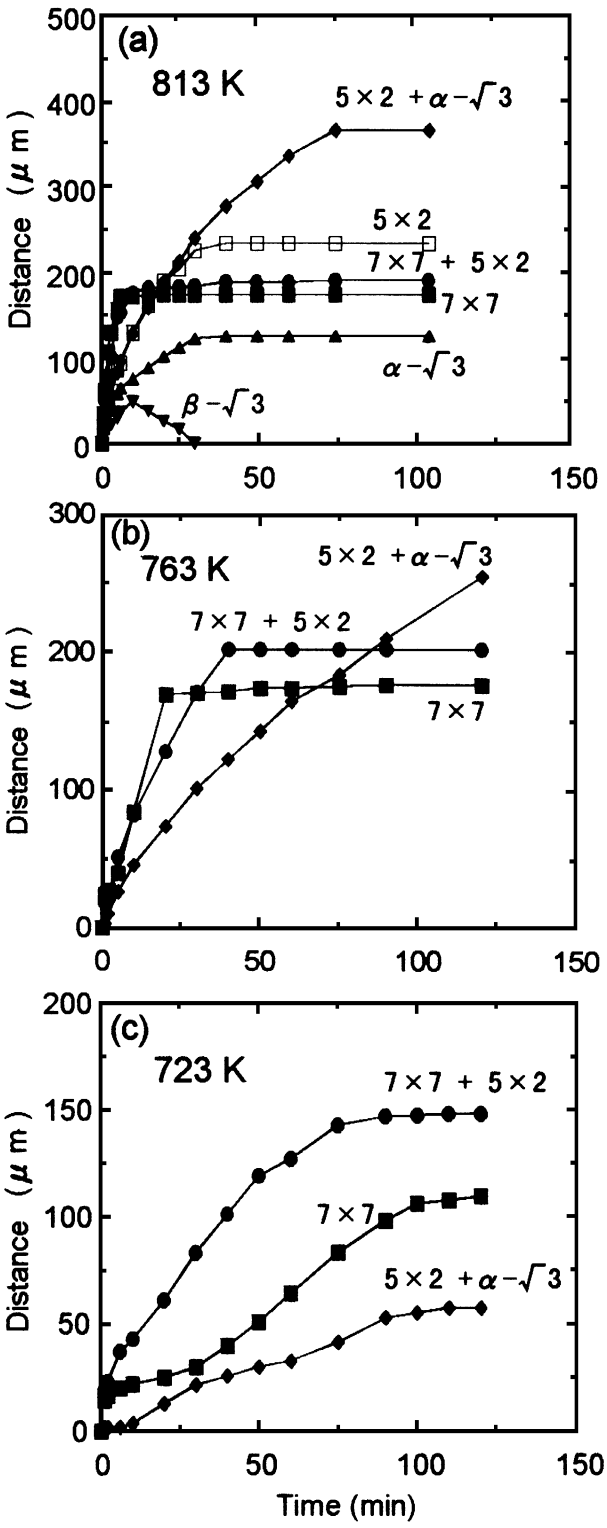

Fig. 3. Migration distance of the front edge of the patch on different substrates as a function of duration of current stressing at (a) 813 K, (b) 763 K, and (c) 723 K. Au coverages and corresponding superstructures on the respective substrates were $(7 \times 7) \sim 0$ ML, $(7 \times 7 + 5 \times 2) \sim 0.36$ ML, $(5 \times 2) \sim 0.49$ ML, $(5 \times 2 + \alpha\text{-}\sqrt{3}) \sim 0.71$ ML, $(\alpha\text{-}\sqrt{3}) \sim 0.79$ ML, and $(\beta\text{-}\sqrt{3}) \sim 1.0$ ML.

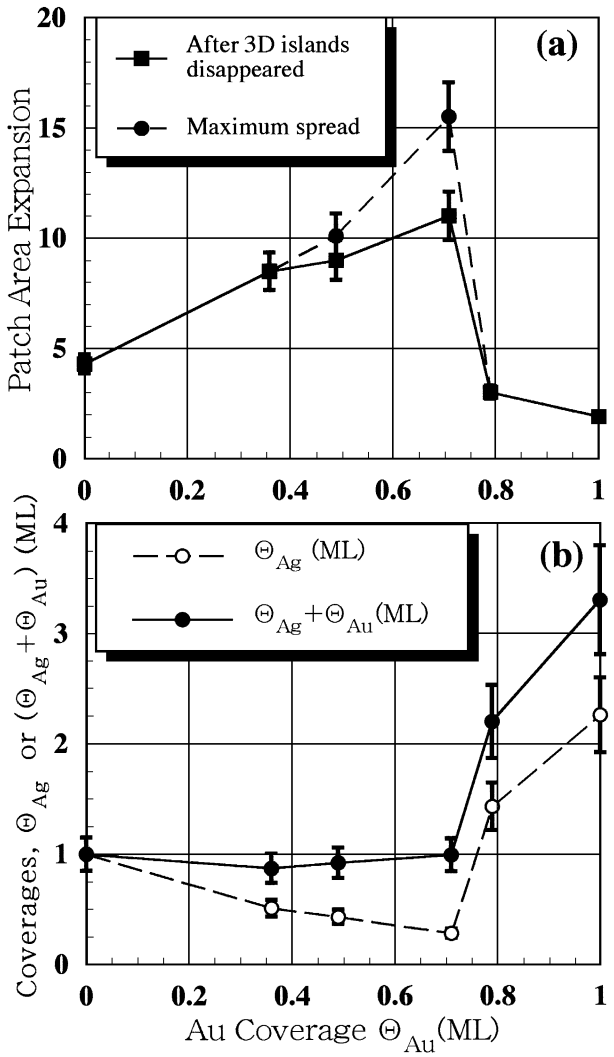

Fig. 4. (a) Expansion of the patch area on the substrates of different Au coverages at 813 K. Solid squares on a solid line represent the expansion of the area measured at the time when 3D islands apparently disappeared, while solid circles on a dashed line show the expansion when the patch area reached its maximum, which nearly coincides with the solid line data except on the 5×2 and ($5 \times 2 + \alpha$-$\sqrt{3} \times \sqrt{3}$) surfaces (b) Ag coverages θ_{Ag} (open circles) and sums of Ag and Au coverages (solid circles) in the final patches after current stressing on the respective substrates are shown as a function of the precovered Au coverage θ_{Au}.

The patches after attaining the maximum spread always showed $\sqrt{3} \times \sqrt{3}$ RHEED patterns, irrespective of Au coverages, which are, however, different in spot intensity distribution from the $\sqrt{3} \times \sqrt{3}$ phase with Ag only (so-called honeycomb-chained triangle (HCT) structure.[16,17]) Hence, it can be said that the patches after spreading are two-dimensional (2D) alloy phase of Ag and Au.

Now, let us estimate the concentrations of Ag and Au in the 2D phase of the respective patches. The average Ag coverage θ_{Ag} over the patch decreases with its expansion while θ_{Au} remains constant. Since, on the 7×7 substrate ($\theta_{Au} = 0$ ML), the final patch is composed of 1 ML Ag, showing the $\sqrt{3} \times \sqrt{3}$-Ag phase of the HCT structure, the average Ag coverages in the patches on the other substrates can be estimated by comparing the respective area expansions with that on the 7×7 substrate. The Ag coverages θ_{Ag} thus estimated are shown by open circles in Fig. 4(b). θ_{Ag} decreases with θ_{Au} up to $\theta_{Au} \sim 0.7$ ML, although it is considerably larger at $\theta_{Au} > 0.8$ ML. The sums of θ_{Ag} and θ_{Au} coverage in the patches on the respective substrates are also shown by solid circles in Fig. 4(b). It is noticed that, up to $\theta_{Au} \sim 0.7$ ML, the sums of Au and Ag coverages in the respective patches are always around 1 ML. Therefore we can say that the final patches attained after current feeding (and resulting heating) are 2D alloy phases with different Ag/Au concentration ratios under a condition of $\theta_{Au} + \theta_{Ag} = 1$ ML. The 2D alloy phase formation with this rule has been already reported during thermal desorption of Ag from the (Au + Ag) co-adsorbed Si(111) surfaces.[18] However, in case of $\theta_{Au} > 0.8$ ML, this rule does not seem to apply. However, the above-mentioned estimates of θ_{Ag} are based on an assumption that no Ag atoms desorb from (or diffuse into) the substrate, which may not be true especially for the substrates of $\theta_{Au} > 0.8$ ML. This is because, as seen in Fig. 3(a), the patch on the β-$\sqrt{3}$ substrate apparently shrank, meaning that Ag atoms disappeared form the substrate surface region during the current stressing. Therefore, we speculate that actual Ag coverages on the substrates of $\theta_{Au} > 0.8$ ML are much lower than those estimated in Fig. 4(b), suggesting an application of the condition of $\theta_{Au} + \theta_{Ag} = 1$ ML on all substrates.

The concentration ratios θ_{Ag}/θ_{Au}, and sums of θ_{Ag} and θ_{Au} in the patches on two substrates were obtained at different temperatures, and are summarized in Fig. 5. On the

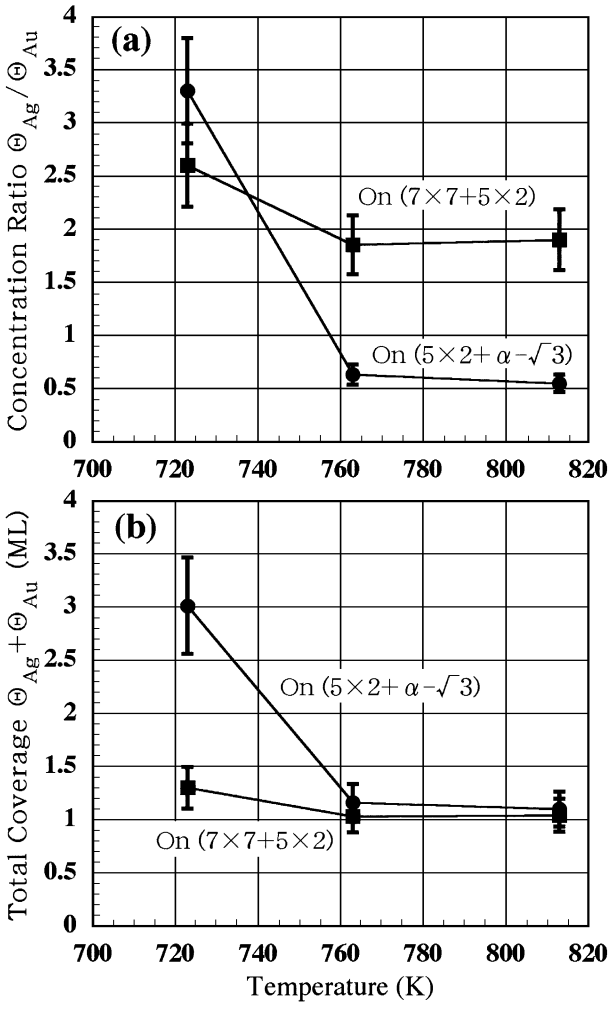

Fig. 5. (a) Concentration ratios θ_{Ag}/θ_{Au}, and (b) sums of θ_{Ag} and θ_{Au} in the respective final patches after electromigration on the ($7 \times 7 + 5 \times 2$) and ($5 \times 2 + \alpha$-$\sqrt{3}$) substrates at differentsubstrate temperatures.

$(7\times7+5\times2)$ surface ($\theta_{Au} \sim 0.36$ ML), a Ag-rich alloy phase ($\theta_{Ag}/\theta_{Au} \sim 2$–$2.5$) is formed irrespective of the temperature, while on the $(5 \times 2 + \alpha\text{-}\sqrt{3})$ surface ($\theta_{Au} \sim 0.71$ ML), the Ag-rich alloy phase at 723 K is transformed into a Au-rich phase ($\theta_{Ag}/\theta_{Au} \sim 0.5$) at higher temperatures. However, at higher temperatures, both substrates give the patches of 2D alloy phase characterized by $\theta_{Au} + \theta_{Ag} = 1$ ML as shown in Fig. 5(b). Thus the final patches are composed of characteristic 2D alloy phases, which is the reason for different spreading ability of the Ag patch on different substrates as observed in Fig. 3. At lower temperatures (723 K in our case), it is considered that thermal energy is not sufficient to form such a stable 2D alloy phase.

Figure 6 shows the Arrhenius plot of Ag electromigration on the different substrates. Flows of Ag-atom flux at the front edge of the respective patches were estimated by the initial spreading speed of the front edge of the patches shown in Fig. 3, taking the above-mentioned average Ag coverages θ_{Ag} in the respective patches also into consideration. These analyses show that the activation energies for the Ag migration on all substrates shown here are similar to each other (∼1.6 eV), while pre-exponential factors are reduced for the Au-adsorbed substrates.

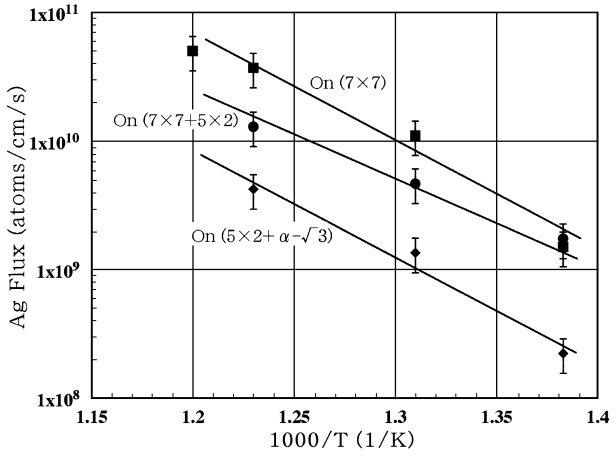

Fig. 6. Arrhenius plot of Ag electromigration on the clean 7 × 7 and Au-covered surfaces. Lateral fluxes of Ag atoms at the front edge of the respective patches were measured from the initial speed of the patch expansion (Fig. 3) and also average Ag concentrations in the respective patches on the different substrates (Fig. 4).

In summary, apparent differences in spreading of the Ag patches are systematically understood by considering the final 2D alloy phases characterized by a rule for concentrations $\theta_{Au} + \theta_{Ag} = 1$ ML, though behaviors of migration and desorption from (diffusion into) the substrates are modified by the precovered Au.

This work has been supported in part by a Grant-in-Aid from the Ministry of Education, Science, Culture, and Sports of Japan, especially for Creative Basic Research (No. 09NP1201) conducted by Professor K. Yagi of Tokyo Institute of Technology. We have also been supported by Core Research for Evolutional Science and Technology of the Japan Science and Technology Corporation conducted by Professor M. Aono of Osaka University and RIKEN.

1) H. Yasunaga and A. Natori: Surf. Sci. Rep. **15** (1992) 205.
2) A. Yamanaka and K. Yagi: Surf. Sci. **242** (1991) 181.
3) H. Yamaguchi, Y. Tanishiro and K. Yagi: Appl. Surf. Sci. **60/61** (1992) 79.
4) K. Anno, N. Nakamura and S. Kono: Surf. Sci. **260** (1992)53.
5) K. Yagi, A. Yamanaka and H. Yamaguchi: Surf. Sci. **283** (1993) 300.
6) Y. Shidahara, K. Aoki, Y. Tanishiro, H. Minoda and K. Yagi: Surf. Sci. **357–358** (1996) 820.
7) T. Ichinokawa, H. Izumi, C. Haginoya and H. Itoh: Phys. Rev. B **47** (1993) 9654.
8) H. Kahata and K. Yagi: Surf. Sci. **220** (1989) 131.
9) M. Ichikawa and T. Doi: Appl. Phys. Lett. **60** (1992) 1082.
10) A. V. Latyshev, A. B. Krasilnikov and A. L. Aseev: Surf. Sci. **311** (1994) 395.
11) T. Doi and M. Ichikawa: Jpn. J. Appl. Phys. **34** (1995) 25.
12) T. Doi, M. Ichikawa and S. Hosoki: Appl. Phys. Lett. **69** (1996) 532.
13) T. Doi, M. Ichikawa, S. Hosoki and K. Ninomiya: Appl. Phys. Lett. **68** (1996) 1493.
14) *e.g.* T. Nagao, S. Hasegawa, K. Tsuchie, S. Ino, C. Voges, G. Klos, H. Pfnur and M. Henzler: Phys. Rev. B **57** (1998) 10100.
15) S. Hasegawa, X. Tong, S. Takeda, N. Sato and T. Nagao: Prog. Surf. Sci. **60** (1999) 89.
16) T. Takahashi, S. Nakatani, N. Okamoto, T. Ishikawa and S. Kikuta: Surf. Sci. **242** (1991) 54.
17) M. Katayama, R. S. Williams, M. Kato, E. Nomura and M. Aono: Phys. Rev. Lett. **66** (1991) 2762.
18) S. Ino, T. Yamanaka and S. Ito: Surf. Sci. **283** (1993) 319.